Supporting Information

For

Polyelectrolyte Multilayers under Compression: Concurrent Osmotic Stress and Colloidal Probe Atomic Force Microscopy

Bo Wu[†‡§], Guangming Liu[†]*, Guangzhao Zhang[§], Vincent S. J. Craig[‡]*

[†]Department of Chemical Physics, Hefei National Laboratory for Physical Sciences at Microscale, University of Science and Technology of China, Hefei, 230026, P. R. China.

[‡]Department of Applied Mathematics, Research School of Physics and Engineering, Australian National University, Canberra, ACT 0200, Australia.

[§]Faculty of Materials Science and Engineering, South China University of Technology, Guangzhou, 510640, P. R. China.

*E-mail: gml@ustc.edu.cn, *E-mail: vince.craig@anu.edu.au

Contents

S1. Preparation of polyelectrolyte multilayers

    A. **Synthesis of photo-cross-linkable polyelectrolyte**

    B. **Fabrication of polyelectrolyte multilayers**

**Table S1.** Layer thickness of the cross-linked and native PEMs in dextran solutions

S2. Analysis of the hydrodynamic component of the interaction

S3. References

S1. Preparation of polyelectrolyte multilayers

A. Synthesis of photo-cross-linkable polyelectrolyte

The synthesis and purification of photo-cross-linkable monomer, 7-methylacryloyloxy-4-methylcoumarin (MAOMC) followed an optimized protocol as described before[1]. The product was confirmed by ^{1}H-NMR (Bruker, 600 MHz, d^6-DMSO, See Fig. S1). Purified MAOMC was copolymerized with SS in DMF by using AIBN as free radial initiator ([MAOMC]:[SS]:[AIBN] = 3:2:0.04). The reaction was carried out at 80 °C for 24 h. The resultant copolymer poly(MAOMC-co-SS) aqueous solution was dialyzed against Millipore-Q water for one week and lyophilized to harvest a white flocculated solid. The composition and molecular weight of the copolymer were characterized by elemental analysis (Vario EL cube, Elementar) and analytical ultracentrifugation (XL-A, Beckman), respectively. The S content and O content was 5.1 wt% and 32.3 wt%, respectively. Thus, composition of the copolymer was [MAOMC]:[SS]=1.7:1. The molecular weight was ~ 3.9×10^4 g·mol^{-1}.
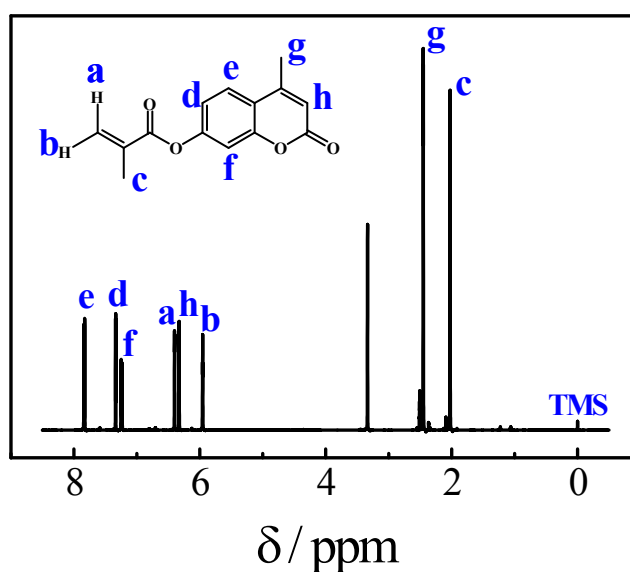
Figure S1 ^{1}H-NMR spectrum of 7-methylacryloyloxy-4-methylcoumarin (MAOMC).

B. Fabrication of polyelectrolyte multilayers

A silicon wafer (Silicon Valley Microelectronics, CA) with ~ 2 nm native oxide layer was used as a substrate for preparation of the polyelectrolyte multilayers. The silica was cleaned with Piranha solution for 20 min at 60 °C, rinsed with plenty of Millipore-Q water, and stored in water until use. Immediately before use the surfaces were rinsed with water and distilled ethanol before being dried under a dry nitrogen stream, then, the wafers were treated with water plasma (Harrick, 18 W, 5 min). This process ensured that the silica surface was fully cleaned and hydroxylated without altering the thickness of the oxide layer.

The cationic polymer CGG and the anionic polymers PSS and poly(MAOMC-co-SS) were dissolved in a 0.1 M NaCl solution at a concentration of 0.1 mg mL^{-1}. In order to minimize the influence of the substrate on the growth of multilayer, the pre-cleaned silicon wafer was first soaked into 1.0 mg mL^{-1} PEI solution for ~ 20 min and a uniform positively charged coating formed on the substrate[2]. The PEM was assembled on the substrate by alternately dipping the substrate for 20 minutes in the PSS and CGG solutions. Between alternate exposures the surface was rinsed three times with 0.1 M NaCl solution for 5 min. In this way, five bilayers of multilayer were assembled, denoted as (PSS/CGG)$_5$. Further layers were adsorbed in order to ultimately produce an outer surface that could be cross-linked. Poly(MAOMC-co-SS) and CGG solution were alternately assembled until 2 bilayers of photo-cross-linkable multilayer were formed. These PEMs are denoted as (PSS/CGG)$_5$[poly(MAOMC-co-SS)/CGG]$_2$. The (PSS/CGG)$_5$[poly(MAOMC-co-SS)/CGG]$_2$ films without exposure

to UV light (native) and after exposure to UV light to induce cross-linking (cross-linked) were studied.

The assembly process of the polyelectrolyte multilayers was tracked using a surface Zeta potential analyzer (Delsa^{TM} Nano C, Beckman). The results are presented in Fig. S2. The thickness of the multilayers in dry state (d_{dry}) was measured by ellipsometry (M-2000V, J. A. Woollam). The photo-cross-linked multilayer was prepared using a UV light generator (Hamamatsu, L9588) employing a wavelength of 365 nm. The kinetics of the cross-linking photoreaction was determined using a UV/visible spectrophotometer (UNICO 2802PCS) with the wavelength range set to 200 nm - 500 nm.
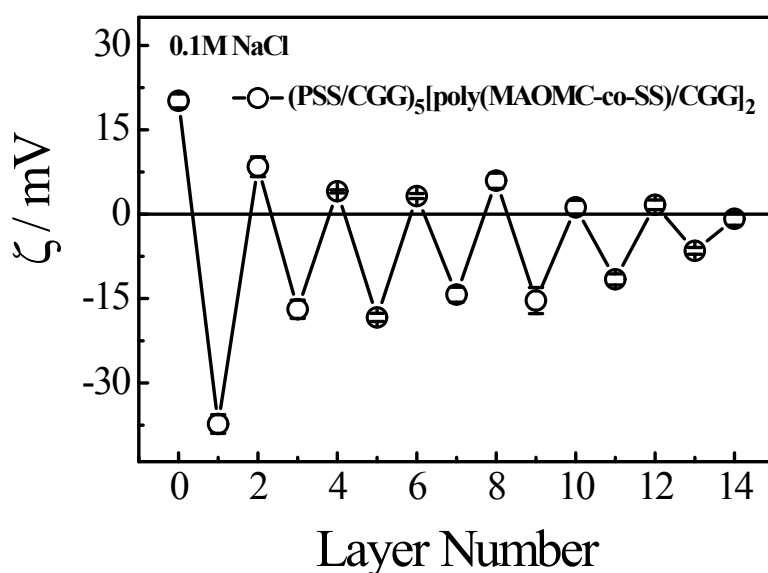

Figure S2 The layer number dependence of change in surface Zeta potential (ζ) for (PSS/CGG)$_5$[poly(MAOMC-co-SS)/CGG]$_2$ multilayer at the NaCl concentration (C_{NaCl}) of 0.1 M. Here, for the 1st layer to the 10th layer, the odd and even layer numbers correspond to the deposition of negatively charged PSS and positively charged CGG, respectively, and for the 11th layer to the 14th layer, the odd and even layer numbers correspond to the deposition of negatively charged poly(MAOMC-co-SS) and positively charged CGG, respectively.

After the exposure to UV light for 30 s, 1 min, 3 min and 5 min. Cross-linking was achieved using irradiation at 365 nm to induce the photoreaction shown in Fig. S3(a). The exposure time needed to be sufficient to ensure full cross-linking yet not so long as to degrade the polymer film as the side groups can photodegrade[3].

The UV-Vis spectra of the polyelectrolyte multilayers consisting of 9 layers (PSS/CGG)$_4$PSS, 10 layers (PSS/CGG)$_5$, 12 layers (PSS/CGG)$_5$[poly(MAOMC-co-SS)/CGG] and 14 layers (PSS/CGG)$_5$[poly(MAOMC-co-SS)/CGG]$_2$ are shown in Fig. S3(b). There is no absorption peak from $\lambda = 250$ nm to 350 nm when the PEM consists only of PSS and CGG. However, when the poly(MAOMC-co-SS) is present, the UV-Vis spectrum shows two broad absorption bands at $\lambda = 276$ and 312 nm which is consistent with the spectrum of polyMAOMC homopolymer in solution. The band at $\lambda = 276$ nm can be attributed to K band absorption caused by the double bonds of the lactone rings in MAOMC, while the band at $\lambda = 312$ nm is caused by the conjugated phenyl groups[1]. The intensity of the two characteristic adsorption peaks is greater for the 14 layer PEM than the 12 layer PEM, showing that photo-cross-linkable layers were fabricated successfully. These characteristic absorption bands allow the photoreaction kinetics of cross-linking to be followed as shown in Fig. S3(c). The intensity of the two characteristic adsorption peaks decreases and disappears after 1 minute of UV irradiation, indicating that the complete cross-linking has been achieved.

The stability of the PEM multilayer cross-linked by 1 min of UV irradiation in dextran solution was studied by ellipsometry. The dry thickness of the multilayer remained unchanged after soaking in 0 wt% (only 0.1 M NaCl), 4 wt%, 10 wt% and 20 wt% dextran solutions overnight. This result shows that 1 min UV irradiation is

sufficient to complete the cross-linking of the PEM's outer layer yet insufficient to cause significant photo-degradation. Therefore 1 min UV irradiation was to effect cross-linking in subsequent experiments.
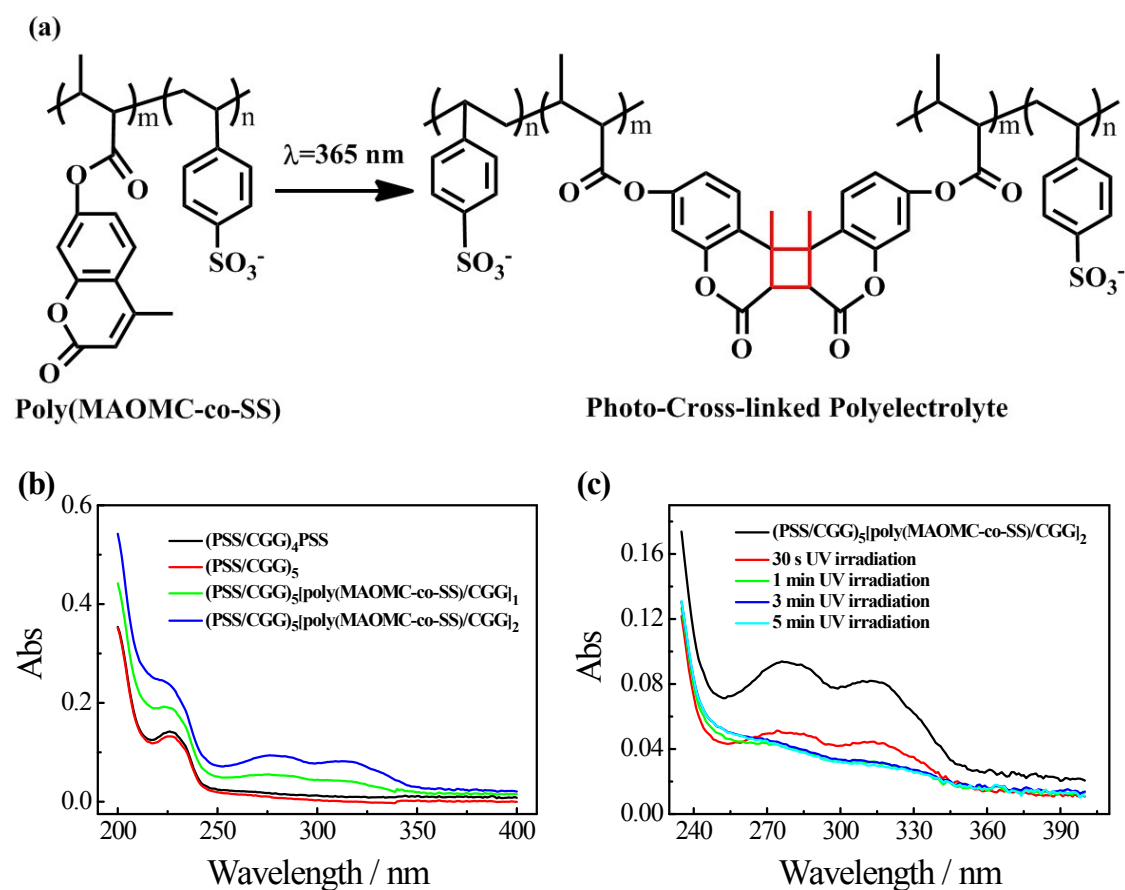
Figure S3 Photoreaction scheme and kinetics. (a) Scheme for photodimerization-induced cross-linking of poly(MAOMC-co-SS) copolymer chains in PEM. (b) UV-Vis spectra of the PEMs with different outer layers. (c) UV-Vis spectra for the photoreaction kinetics of $(PSS/CGG)_5[poly(MAOMC-co-SS)/CGG]_2$ multilayer.

Table S1. Layer thickness of the cross-linked and native PEMs in dextran solutions

	Layer thickness (nm)	
Dextran (wt%)	Cross-linked PEM	Native PEM
20	~ 111	~ 92
10	~ 126	~ 116
4	~ 146	~ 136
0	~ 167	~ 146

## S2. Analysis of the hydrodynamic component of the interaction

Here we analyse the hydrodynamic component of the interaction measured in the absence of Dextran between the cross-linked PEM multilayer, this corresponds to the data in Fig. 3a (0 wt% Dextran) and in Fig. 6 (0 wt% Dextran).

It is not a simple matter to determine the hydrodynamic component for a number of reasons. Firstly it is unclear where the zero of separation for the hydrodynamic contribution should be set. One can estimate this as a position within the outer region of the PEM[4]. Then the further assumption is required that the shear plane does not change during the interaction. Further, the segment density of the polymer is changing with separation, such that the viscosity is a function of separation. We ignore the fact that the viscosity within the gap between the surfaces is likely not uniform, as this would complicate the calculations significantly. We also assume a no-slip boundary condition. Furthermore, the deflection of the spring changes with separation due to

the interaction forces, this changes the velocity of approach during a measurement, even if the piezo velocity is constant.

Our approach is to start with the Pressure versus Separation data for the 0 Wt % dextran solution and subtract the equilibrium curve (see Fig. 6 in the main paper) to obtain the dynamic component of the pressure this is shown in Fig S4. Note that there is some noise in the experimental data evident at low values of the pressure, P.
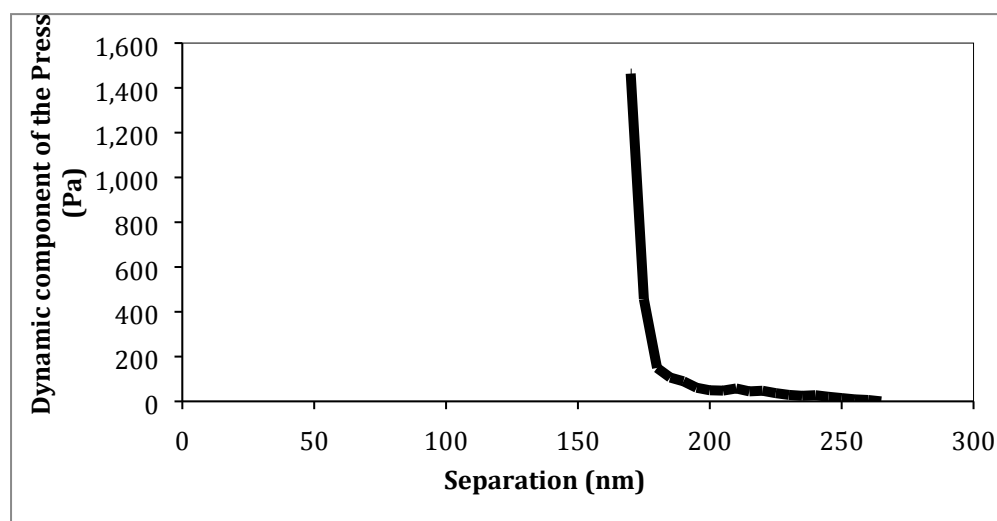
Figure S4. The dynamic component of the measured pressure versus separation between the cross-linked multilayer a borosilicate sphere ($\sim$ 10 μm in radius) and the PEM in the presence of 0 wt% dextran at an approach rate of 40 nm s^{-1}.

The data is then converted to F/R versus separation as per equation S1[5]

$$P = \frac{-1}{2\pi}\frac{d(F/R)}{dD} \qquad (S1)$$

This is then converted to F versus separation by multiplying by the sphere radius R. This gives the dynamic component of the measured force in Fig. S5. Here the noise

in the data at low values of the pressure seen in Fig. S4 contributes little and therefore has little effect on the data in Fig. S5.
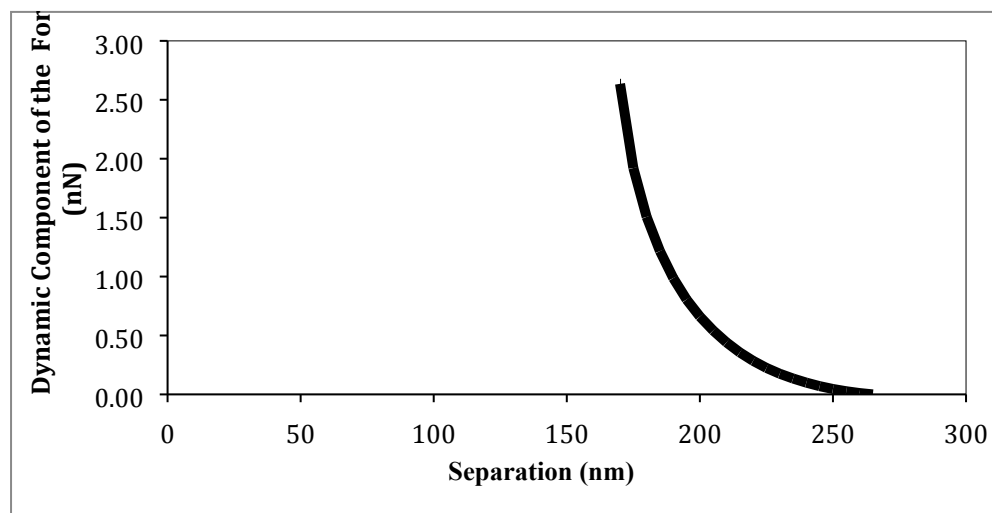
Figure S5. The calculated dynamic component of the measured force versus separation between the cross-linked multilayer a borosilicate sphere ($\sim$ 10 µm in radius) and the PEM in the presence of 0 wt% dextran at an approach rate of 40 nm s^{-1}.

The hydrodynamic drag force F_H, on a sphere of radius R, approaching a wall with velocity dh/dt, in a fluid of viscosity η, at a distance a between the center of the sphere and the wall is given exactly by Brenner[6] for low Reynolds number flow (<1). When the distance between the surface of the sphere and the wall, h (where $h = a - R$), is small compared to the radius of the sphere, R, Brenner's equation can be accurately approximated by the following equation S2; [7, 8]

$$F_H = \frac{6\pi\eta R^2\frac{dh}{dt}}{h} \qquad\qquad (S2)$$

If we then make the assumption that the dynamic component of the force is due wholly to hydrodynamics, the effective viscosity as a function of separation can be determined from Equation S3.

$$\eta = \frac{h\,F_H}{6\pi\eta R^2 \dfrac{dh}{dt}}$$

(S3)

Here the actual approach velocity of the surfaces (dh/dt) changes as a function of separation and is therefore calculated at each separation from the measured data by taking into account the change in deflection of the cantilever and the ramp velocity. The hydrodynamic separation, h, is different to the surface – surface separation, and is measured with respect to the shear plane, which is estimated to be at a surface separation of 159 nm, (this should be compared to the separation between the surfaces when the PEM's are highly compressed which is ~ 168 nm). We have a chosen a value within the PEM in line with earlier work that showed the hydrodynamic shear plane lay within the polymer film for a polymer brush[4]. In Fig. S6, the viscosity is plotted in units of cP (rather than the SI units of Pa.s: note 1 cP= 1 mPa.s) to allow for easy comparison to the viscosity of water, which is 1.002 cP at 20° C.
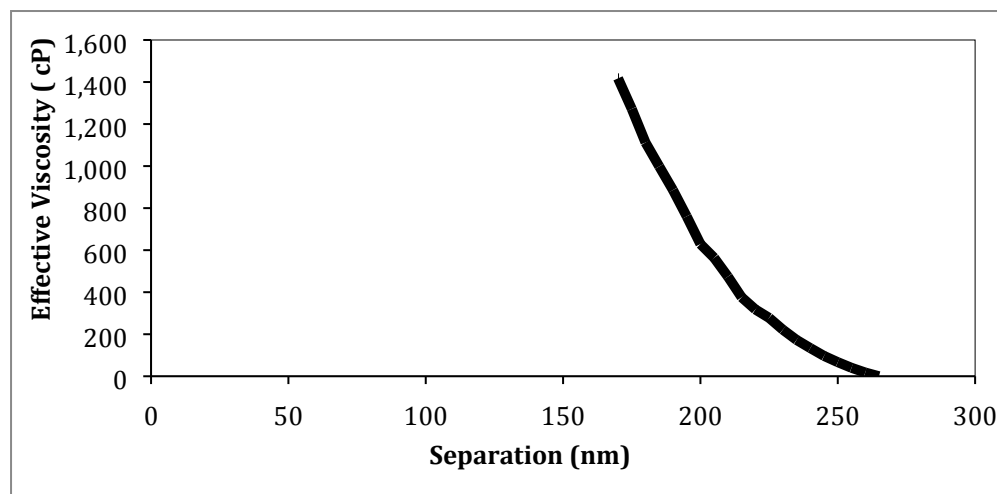
Figure S6. The calculated effective viscosity versus separation between the cross-linked multilayer a borosilicate sphere ($\sim$ 10 μm in radius) and the PEM in the presence of 0 wt% dextran at an approach rate of 40 nm s^{-1}. The calculation is made assuming the shear plan is located at a surface separation of 159 nm, which is 9 nm within the compressed PEM.

It can be seen that the effective viscosity of the mixture of solvent and PEM chains rapidly rises from that of water at large separation to a value about 1300 times that of water when the PEM's are highly compressed. Note that the viscosity values are only an estimate as they strongly depend on the choice of the position of the shear plane. However, if the shear plane is moved further away from the surfaces (reducing the calculated viscosity) we obtain the unphysical result that the viscosity passes through a maximum and then reduces as the surfaces are compressed. The effect of moving the shear plane further into the compressed polymer film is to increase the effective viscosity. The calculated increase in viscosity is comparable to the shear viscosity of polyelectrolyte multilayers of similar thickness determined from fitting of QCM data (270 cP) [9] noting that this is for a different system and is an average value for an uncompressed film. Additionally the high frequency QCM measurements are more likely to elicit an elastic response.

S6. References

1. Y. Chen and J.-D. Wu, *Journal of Polymer Science Part A: Polymer Chemistry*, 1994, **32**, 1867-1875.
2. E. Poptoshev, B. Schoeler and F. Caruso, *Langmuir*, 2004, **20**, 829-834.
3. S. R. Trenor, A. R. Shultz, B. J. Love and T. E. Long, *Chemical Reviews*, 2004, **104**, 3059-3078.
4. S. C. McLean, H. Lioe, L. Meagher, V. S. J. Craig and M. L. Gee, *Langmuir*, 2005, **21**, 2199-2208.
5. V. A. Parsegian, R. P. Rand and N. L. Fuller, *The Journal of Physical Chemistry*, 1991, **95**, 4777-4782.
6. H. Brenner, *Chemical Engineering Science*, 1961, **16**, 242-251.
7. G. D. Mackay and S. G. Mason, *Journal of Colloid Science*, 1961, **16**, 632-&.
8. G. D. M. Mackay, M. Suzuki and S. G. Mason, *Journal of Colloid Science*, 1963, **18**, 103-&.
9. T. T. M. Ho, K. E. Bremmell, M. Krasowska, D. N. Stringer, B. Thierry and D. A. Beattie, *Soft Matter*, 2015, **11**, 2110-2124.